15 May 1998

ELSEVIER

Chemical Physics Letters 288 (1998) 124–130

CHEMICAL PHYSICS LETTERS

Total cross-sections of electron and positron collisions with CHF_3 molecules: a comparative study with CH_4 and CF_4

Osamu Sueoka [a], Hideki Takaki [a], Akira Hamada [b], Hiroshi Sato [c], Mineo Kimura [d,e]

[a] *Faculty of Engineering, Yamaguchi University, Ube, Yamaguchi 755, Japan*
[b] *Department of Physics, Yamaguchi University, Yoshida, Yamaguchi 753, Japan*
[c] *Department of Information Sciences, Ochanomizu University, Tokyo 112, Japan*
[d] *School of Medical Sciences, Yamaguchi University, Ube, Yamaguchi 755, Japan*
[e] *Institute of Space and Astronautical Science, Sagamihara, Kanagawa 229, Japan*

Received 13 September 1997; in final form 19 February 1998

Abstract

Total cross-sections for electron (e^-) and positron (e^+) scattering from CHF_3 have been measured from 0.7 to 600 eV and compared with the theoretical elastic cross-section. For e^- scattering, the cross-sections are found to be larger by 30% than the data compiled by Christophorou et al. [L.G. Christophorou, J.K. Olthoff, M.V.V.S. Rao, J. Phys. Chem. Ref. Data 26 (1997) 1] in the entire energy range measured, but their energy dependence is in good agreement. For e^+ scattering, the cross-sections are smaller by at least a factor of two than those for electron scattering below 20–30 eV, but quickly approach those of electron impact beyond 100 eV. A comparative study with CH_4 and CF_4 reported in our previous papers provides detailed information on the dynamics.

1. Introduction

Due to the basic importance for fundamental understanding of electronic structures and scattering processes and for applications in various fields, particularly in plasma processing, a study on the total, elastic and inelastic processes for electron scattering from trifluoromethane (CHF_3) has attracted much interest in recent years [1]. Its short lifetime in stratosphere means that this molecule has a potential application in plasma processing as a next-generation process gas [2]. Therefore, it is essential to establish all cross-section data for electron scattering of this molecule by compiling existing experimental and theoretical results. Further, a comparative study of electron and positron scattering is expected to provide deeper insight in the fundamental aspects of atomic and molecular dynamics in hydrocarbons and interaction mechanisms. Therefore, we have carried out a comparative examination on the collision from CH_4, CHF_3 and CF_4 molecules.

There is an experimental study in which momentum transfer cross-sections by electron impact have been measured [3] and a combined experimental and theoretical study on differential cross-sections by electron impact for all fluoromethanes [4]. Here a complete study of total cross-sections (TCSs) based on both electron and positron scattering has been carried out. We have initiated the present joint experimental and theoretical investigations on these processes for CHF_3 to provide comprehensive TCSs for assessing magnitudes of other weak inelastic chan-

0009-2614/98/$19.00
PII: S0009-2614(98)00247-4

nels as well as dynamical information for deriving guiding principle for applications to other fluoromethanes [4].

2. Experimental and theoretical apparatus

The experimental apparatus and the method have been reported earlier [5–8]. A ^{22}Na radioisotope of 90 μCi and baked tungsten ribbons were used as the positron source and the positron moderator for low-energy particles, respectively. For the electron source, slow electron beams (with an energy width of ~1 eV) were produced after secondary electrons, which were emitted from the same isotope, were moderated by multiple scattering in the tungsten ribbons. The apparatus for the TCS measurement used for electron and positron impacts was a straight type time-of-flight (TOF) system. A schematic diagram of the experimental arrangement is shown in Fig. 1. A retarding potential unit was combined to the TOF system for elimination of elastically and inelastically scattered projectiles. The purity of the CHF_3 gas was 99.995%.

TCS values Q_t are given by

$$Q_t = -(1/nl)\ln(I_g/I_v), \quad (1)$$

where n and l are the gas density in the collision cell and the effective length of the cell, respectively, and I_g and I_v are the beam intensity in the gas and vacuum, respectively. The effective length of the cell was derived by normalizing the TCSs to those in the positron–N_2 data of Hoffman et al. [9]. The pressure independence of the TCS were confirmed by electron scattering at 5 and 6 eV.

The forward scattering due to the magnetic field and a large collision-cell aperture in the experiment should be distinguished from that of the unscattered beam and the correction for this effect should be included in the data analysis as previously described [10], where a simulation of each projectile under the conditions of geometry, external field and scattering conditions was carried out to estimate the correction by examining if the projectile came through the scattering chamber. The same procedure for estimation of the correction was followed in the present study. The differential cross-section data for this correction, both for electron and positron scattering, were obtained from the present theoretical results. The correction for electron scattering amounts to 10–17% below 70 eV, but it becomes much smaller at higher energies to < 5% above 200 eV. For positron scattering, the corrections are generally found to be slightly larger than those for electron scattering. The forward-scattering correction described above is included in all the data presented in Table 1.

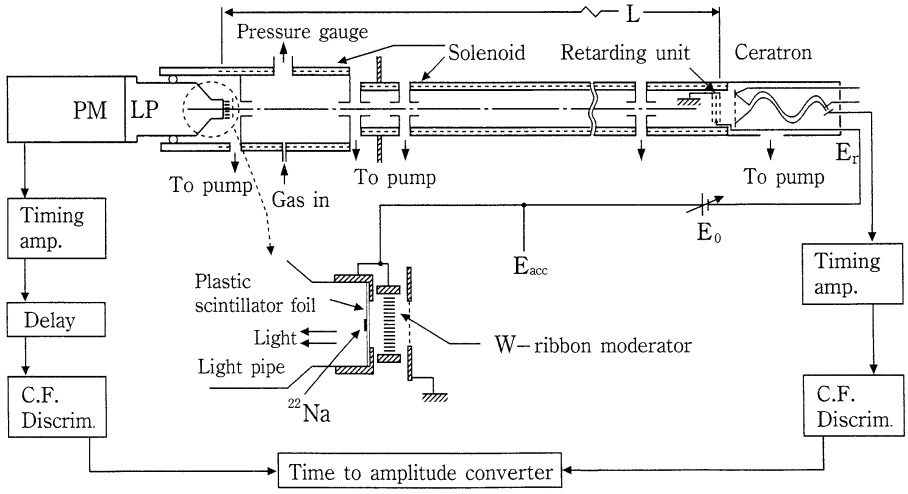

Fig. 1. A schematic diagram of the present experimental apparatus. The symbols, PM, LP, E_r, E_{acc}, E_0 and C.F. Discrm. are the photomultiplier, light pipe, retarding energy, acceleration energy, constant energy ($E_0 = E_{acc} - E_r$) and constant fraction discriminator, respectively.

Table 1
Numerical data of the experimental total cross-sections[a]

E (eV)	$\sigma_{tot}(e^-)$ (10^{-16} cm^2)	$\sigma_{tot}(e^+)$ (10^{-16} cm^2)
0.7	–	13.1 ± 0.7
0.8	32.1 ± 1.1	–
1.0	30.2 ± 1.0	13.6 ± 0.7
1.2	29.5 ± 1.0	–
1.3	–	14.6 ± 0.7
1.4	29.2 ± 1.0	–
1.6	28.9 ± 1.0	14.2 ± 0.7
1.8	28.4 ± 1.0	–
1.9	–	14.1 ± 0.7
2.0	27.4 ± 1.0	–
2.2	26.4 ± 0.9	13.5 ± 0.6
2.5	25.9 ± 0.8	12.4 ± 0.6
2.8	25.6 ± 0.8	12.4 ± 0.6
3.1	24.5 ± 0.8	11.6 ± 0.6
3.4	24.0 ± 0.9	11.6 ± 0.6
3.7	23.9 ± 0.9	11.3 ± 0.6
4.0	24.1 ± 0.8	11.0 ± 0.5
4.5	24.6 ± 0.8	11.1 ± 0.5
5.0	24.4 ± 0.9	10.5 ± 0.5
5.5	24.8 ± 0.9	10.4 ± 0.5
6.0	26.2 ± 0.9	10.3 ± 0.5
6.5	26.9 ± 0.9	10.3 ± 0.5
7.0	26.3 ± 0.9	10.2 ± 0.5
7.5	26.6 ± 0.9	10.1 ± 0.5
8.0	26.7 ± 0.9	10.1 ± 0.5
8.5	26.8 ± 0.9	10.2 ± 0.5
9.0	26.5 ± 0.9	10.3 ± 0.4
9.5	25.7 ± 0.9	10.6 ± 0.4
10.0	25.2 ± 0.9	10.5 ± 0.4
11.0	23.8 ± 0.8	10.7 ± 0.4
12	23.2 ± 0.9	10.9 ± 0.4
13	22.9 ± 0.8	11.3 ± 0.4
14	22.9 ± 0.8	11.2 ± 0.4
15	22.8 ± 0.8	11.4 ± 0.4
16	22.8 ± 0.8	11.5 ± 0.4
17	22.4 ± 0.8	11.5 ± 0.4
18	22.9 ± 0.8	11.8 ± 0.6
19	23.2 ± 0.8	11.9 ± 0.7
20	23.2 ± 0.8	12.1 ± 0.6
22	23.5 ± 0.8	12.4 ± 0.6
25	23.1 ± 0.8	12.3 ± 0.6
30	23.0 ± 0.8	12.8 ± 0.6
35	22.3 ± 0.8	–
40	21.5 ± 0.8	12.8 ± 0.6
45	18.0 ± 0.6	–
50	20.3 ± 0.7	12.3 ± 0.6
60	19.8 ± 0.7	12.3 ± 0.6
70	18.6 ± 0.7	12.0 ± 0.6
80	17.5 ± 0.6	11.9 ± 0.6
90	16.3 ± 0.6	11.1 ± 0.6
100	15.5 ± 0.6	10.8 ± 0.6
120	13.7 ± 0.5	10.2 ± 0.6
150	12.7 ± 0.5	9.9 ± 0.6
200	10.7 ± 0.4	8.5 ± 0.5
250	9.5 ± 0.4	8.3 ± 0.5
300	8.7 ± 0.3	7.1 ± 0.4
400	7.3 ± 0.3	6.3 ± 0.4
500	6.2 ± 0.3	5.2 ± 0.4
600	5.6 ± 0.2	4.7 ± 0.4

[a] See text for experimental uncertainties.

For assessing the experimental errors (except for the forward-scattering correction), the relative error is estimated by summing all contributions from the intensity, $\Delta I/I$ ($< 1\%$ for electron and 2–4% for positron) where I represents $\ln(I_g/I_v)$, the gas density $\Delta n/n$ ($= 0.3\%$) and the effective length of the cell $\Delta l/l$ ($= 2\%$). The error arising from subtraction of the accidental coincidences in each channel is also included in the statistical errors.

The theoretical approach employed is the continuum multiple-scattering (CMS) method, which is a simple but efficient model for treating electron scattering from polyatomic molecules [11]. To overcome difficulties arising from: (i) the many degrees of freedom of electronic and nuclear motions and (ii) the nonspherical molecular field in a polyatomic molecule, the CMS divides the configuration space into three regions: Region I, the atomic region surrounding each atomic sphere (spherical potentials), Region II, the interstitial region (a constant potential) and Region III, the outer region surrounding the molecule (a spherical potential). The scattering part of the method is based on the static-exchange-polarization potential model within the fixed-nuclei approximation. The static interaction is constructed by the electron density obtained from the CMS wavefunction and the Hara-type free-electron gas model [11] is employed for the local-exchange interaction, while the polarization interaction is considered for only terms proportional to r^{-4}. A simple local exchange potential replaces the cumbersome non-local exchange potential making the practical calculation tractable.

Under these assumptions, the Schrödinger equation in each region is solved numerically under separate boundary conditions. By matching the wavefunctions and their derivatives from each region, we can determine the total wavefunction of the scattered electron and hence, the scattering *S*-matrix. Once the *S*-matrix is known, then the scattering cross-section can be easily calculated. This approach has been tested extensively and is known to provide useful information on the underlying scattering physics [11]. Further, the CMS method is useful for interpolation and extrapolation for guiding experimental data points.

3. Results

3.1. Total cross-section for CHF_3

Fig. 2 presents TCSs for both electron and positron impacts from 0.7 to 600 eV and numerical data of the measurement are given in Table 1. New aspects can be summarized as follows:

(i) The energy dependence of both electron and positron cross-sections are rather weak with small structures around 7–10 eV. The positron cross-section is always smaller than that of electron scattering in the energy range studied. The difference between these two cross-sections is enhanced by a factor of two below a few tens of eV.

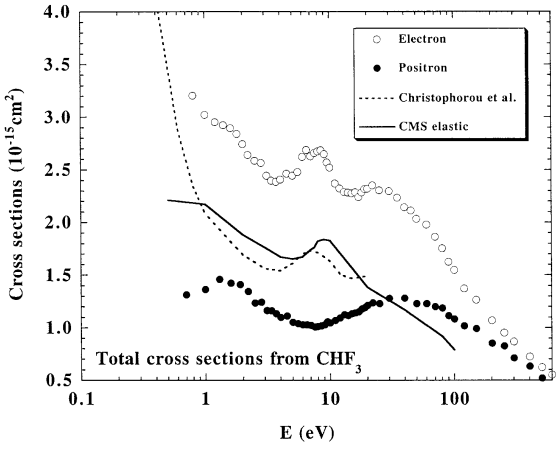

Fig. 2. Total cross-sections for CHF_3 molecule by electron (○) and positron (●) impacts. The dashed line represents the recommended cross-section for electron scattering by Christophorou et al. [1]. The solid line is the present theoretical elastic cross-section for electron scattering based on the CMS method.

(ii) The cross-section by electron impact has two small, broad peaks around 8 and 25 eV due to shape resonances of t_2 and e symmetries, while that of positron impact increases ~ 8 eV due to positronium formation, followed by direct ionization around 15 eV.

(iii) The cross-section by positron impact has a broad minimum around 8 eV, contrary to the electron impact case, with a slight increase at much smaller energy.

(iv) The cross-section by positron impact appears to decrease below 2 eV, while that for electron impact increases in the same energy region. The increase below 2 eV for electron impact can be interpreted as due to the effect of the long-range dipole interaction. The Born formula is known to be valid for describing total and momentum-transfer cross-sections reasonably well for a polar molecule with a medium size of the dipole moment at intermediate energies and gives

$$\sigma_{\mathrm{tot}} \approx \left(f(D)/v^2 \right), \qquad (2)$$

where $f(D)$ is a function of the dipole moment D of a molecule ($D = 1.6$ au for CHF_3) and v is the speed of electron. Obviously, it should increase as the inverse of the collision energy. In fact, this formula was employed to estimate the momentum transfer cross-section in Ref. [2]. Note that momentum-transfer is the dominant process below the vibrational-excitation threshold of a few tenths of eV. Both electron and positron should obey this Born formula in a certain low-energy region, in which both cross-sections eventually increase with lowering energy. Hence, for positrons the experimental energy region studied may still seem to be too high since no increasing trend of the cross-section has been observed.

(v) Both cross-sections appear to merge beyond 200 eV, the reason being apparent from the Born argument.

We include in Fig. 2 the data recommended by Christophorou et al. [2] and the elastic cross-section obtained by the CMS method both for electron scattering. The agreement of the energy dependence between the present measurement and that of the recommended data is excellent, but the present ex-

perimental data are larger by 30% than the recommended data. Therefore, we believe that the recommended values, which were determined by compiling and critically assessing the published data, should be used with care as far as the magnitude is concerned. For positron scattering, there is no other experimental or theoretical data available and hence, no comparison is possible. The present CMS calculation reveals that the shape resonances seen for electron impact are due to t_2 and e symmetries with the peaks at 8 eV and, to a much lesser extent, at 25 eV, respectively. The resonance peak at 25 eV is found to be weaker in the theory than in the experiment. The present treatment for the polarization potential may perhaps be less adequate for describing the magnitude of all resonances. The present theoretical result for elastic cross-section agrees reasonably well with the total cross-section recommended by Christophorou et al. [2], supporting our claim that the recommended cross-section appears to be underestimated. It may be noted that the energy which results in the peak in electron scattering and the dip in positron scattering is exactly the same at 7–8 eV. The reason for this phenomenon awaits large-scale structure and dynamical calculations, but the opposite signs of the static interactions for electron and positron scatterings seem to be responsible.

3.2. Comparative study with CH_4, CHF_3 and CF_4

For understanding of the scattering dynamics and electronic structure, the total cross-sections by electron and positron impacts for CH_4 and CF_4 [5–8] are compared as shown in Fig. 3.

First, we discuss the results by electron impact in Fig. 3a. Beyond $\sim$100 eV, the order of the cross-sections is $CF_4 > CHF_3 > CH_4$. This order is naturally a reflection of the molecular size, since scattering at high energy is dominated by the static potential and hence the scattered electron sees the target charge distribution. As the energy decreases to $\sim$10 eV, the results become $CH_4 \approx CHF_3 > CF_4$, but the peak around 25 eV for CHF_3 is also observed for CF_4. Below $\sim$6 eV, the cross-section for CH_4 drops sharply toward the Ramsauer–Townsend (RT) minimum at 0.4 eV [5,6] and similarly, that for CF_4 decreases slowly toward the RT minimum near 0.15 eV [7,8]. The presence of these RT minima for both

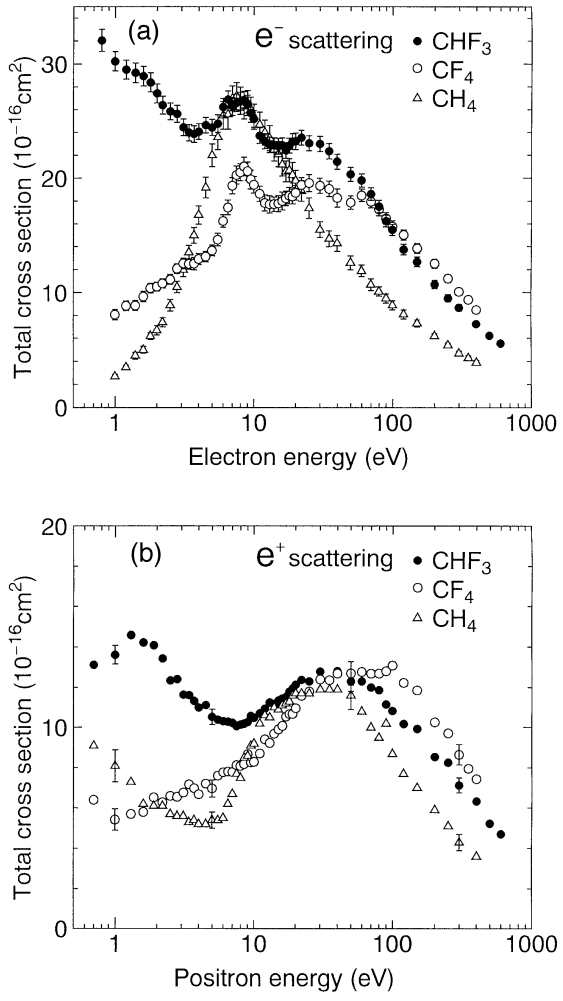

Fig. 3. Total cross-sections for CH_4, CHF_3 and CF_4 by: (a) electron and (b) positron impacts. The results for CH_4 and CF_4 are from Refs. [6,8], respectively.

systems was first observed experimentally and was then confirmed theoretically. In contrast, the cross-section for CHF_3 keeps increasing due to the long-range dipole interaction as stated earlier.

For positron impact shown in Fig. 3b, the magnitudes of the cross-section follow the same order, $CF_4 > CHF_3 > CH_4$ above 50–60 eV for the same reason. The cross-sections for CH_4 and CF_4 show a broad peak around 30–40 and 40–100 eV, respectively; according to Kauppila and Stein [12], this peak is due to a combination of positronium formation near 7 eV and direct ionization near 14 eV. The

peak for CHF_3 at 30–40 eV is apparent, being similar in nature to those of CH_4 and CF_4; another peak at 1.5–2 eV is found to be stronger than those for other molecules. The cross-section for CH_4 shows a minimum at 5 eV and increases at much lower energies. For CF_4, a similar minimum seems to occur at lower energy, ~ 1 eV. For CHF_3, there is a second peak at 2 eV and decreases below 1.5 eV, as stated above. According to the Born argument, it should get back at lower energy because of the dipole interaction. In the present experiment, however, the energy region studied does not seem to be low enough to observe this turnover. The origin of the second peak is not clear at present, but it may well be a resonance (positronium-in-molecule) [13] or anomalously large cross-section for rovibrational excitation [14]. A study of these points is needed along with a search for a similar second peak for CF_4 and CH_4 to have an RT minimum in positron impact, but the present energy region may be still too high to observe the minimum.

In order to better understand the above-mentioned features, an ab initio calculations by GAMESS [15] based on the self-consistent field method have been carried out to examine electronic structures and orbital energies. The results obtained are shown in Fig. 4. Note that we have fixed molecular geometries at each equilibrium position in the calculation. All molecular orbitals with negative and positive energies are occupied and unoccupied orbitals, respectively. All unoccupied molecular orbitals (UMOs) for most molecular targets are known to cause shape-resonances, which are often seen as a broad hump in the cross-section in the neighborhood of a few to a few tens of eV. All orbital energies of low-lying UMOs below 20 eV are included in the figure. For CH_4, UMOs near the resonance-peak at 8 eV correspond to 11.0 and 11.94 eV, while for CHF_3, 9.51, 10.94, 11.5 and 11.6 eV. For CF_4, UMOs near the 8 eV resonance are 9.24, 10.99 and 12.05 eV. These orbitals are responsible for the resonance peaks for all these molecules. Additional UMOs around 9–12 eV for CHF_3 are due to a combination of those from H and F atoms, causing a somewhat stronger resonance peak. These a_1, t_2 and e resonances are observed experimentally above a few eV, in agreement with the present calculations. This orbital argument is valid for providing a rationale for the feature of another resonance-like peak seen around 25 eV. For higher UMOs, we expect that the corresponding resonances are present, even if they are too weak and broad to be visible in the present results. When only one H atom in CH_4 is replaced by an F atom, we have observed a clear difference at higher UMOs, indicating a strong F-atom effect [4]. This difference can be ascribed to a substantial difference in the charge distribution and in the atomic size. Replacement of three F atoms makes CHF_3 nearly identical to CF_4 in the electronic structure, which is apparent from close similarity in the TCSs between CHF_3 and CF_4, supporting our previous argument [4] on a weak contribution to scattering from the H atom.

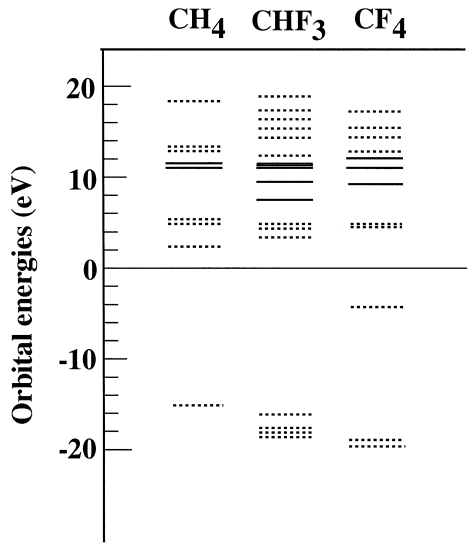

Fig. 4. Orbital energies for CH_4, CHF_3 and CF_4. The solid lines are energies closely lying to the position of the resonance peak around 8 eV, in contrast to dashed lines for energies lying far apart.

In summary, we have measured the total cross-section for CHF_3 by electron and positron impacts from 0.7 to 600 eV. The cross-section for electron impact is larger than that for positron impact below 600 eV and both cross-sections have weak and broad structures below 60 eV. We have provided a rationale for the structures observed. A comparative study of the TCSs for CH_4, CHF_3 and CF_4 reveals a significant effect of F atoms to scattering processes and detailed dynamics, which cause the results for

CH_4 to be substantially different from those for CHF_3 and CF_4.

Acknowledgements

The work has been supported in part by a grant-in-aid from the Ministry of Education, Science and Culture and the Institute of Space and Astronautical Science.

References

[1] L.G. Christophorou, J.K. Olthoff, M.V.V.S. Rao, J. Phys. Chem. Ref. Data 25 (1996) 1341.
[2] L.G. Christophorou, J.K. Olthoff, M.V.V.S. Rao, J. Phys. Chem. Ref. Data 26 (1997) 1.
[3] J. Sanabia, J. Moore, cited in Ref. [2].
[4] H. Tanaka, T. Masai, M. Kimura, T. Nishimura, Y. Itikawa, Phys. Rev. A 56 (1997) R3338.
[5] J. Ferch, B. Granitza, W. Raith, J. Phys. B 18 (1985) L445.
[6] O. Sueoka, S. Mori, J. Phys. B 19 (1986) 4035.
[7] A. Mann, F. Linder, J. Phys. B 25 (1992) 533.
[8] O. Sueoka, S. Mori, A. Hamada, J. Phys. B 27 (1994) 1453.
[9] K.R. Hoffman, M.S. Dababneh, Y.-F. Hsieh, W.E. Kauppila, V. Pol, J.H. Smart, T.S. Stein, Phys. Rev. A 25 (1982) 1393.
[10] A. Hamada, O. Sueoka, J. Phys. B 27 (1994) 5055.
[11] M. Kimura, H. Sato, Comment At. Mol. Phys. 26 (1991) 333.
[12] W. Kauppila, T.S. Stein, in: D. Bates, B. Bederson (Eds.), Adv. At. Mol. Opt. Phys., vol. 26, Academic Press, New York, 1989, p.1.
[13] M. Kimura, O. Sueoka, A. Hamada, M. Takekawa, Y. Itikawa, H. Tanaka, L. Boesten, J. Chem. Phys. 107 (1997) 6616.
[14] M. Kimura, M. Takekawa, Y. Itikawa, Phys. Rev. A (1998) in press.
[15] GAMESS is the package of the ab initio molecular structure calculation written by M.W. Schmidt, K.K. Baldridge, J.A. Boatz, S.T. Elbert, M.S. Gordon, J.H. Jensen, S. Koseki, N. Matsunaga, K.A. Nguyen, S.J. Su, T.L. Windus, M. Dupuis, J.A. Montgomery, J. Comput. Chem. 14 (1993) 1347.